Research article Available online www.ijsrr.org ISSN: 2279–0543

International Journal of Scientific Research and Reviews

Physico-chemical characterization of biochar derived from different raw materials

Varinder Kaur and Praveen Sharma*

Research scholar, Department of Environmental Science and Engineering, Guru Jambheshwar University, Hisar, Contact No. 01662-263153, Haryana, India
(E.mail- varinder.kaur265@gmail.com)
*Professor, Department of Environmental Science and Engineering, Guru Jambheshwar University, Hisar, Contact No. 01662-263153, Haryana, India
(E.mail- ps.enbt@gmail.com)

ABSTRACT

A sustainable solution of biomass burning by converting agricultural and forest residues into biochar is an environment friendly approach. The characteristic of biochar mainly depends on the production temperature and feedstock type. This paper summarizes the results analysed by the different experiments on biochar characteristics. To design the satisfactory conditions for the production of biochar having desired characteristics thus requires understanding of dependencies and affecting factors, both qualitatively and quantitatively. In this investigation, biochar was prepared from *Prosopis juliflora* and mixed wood raw materials. Both chars were obtained by slow pyrolysis at 450°C by using traditional earth mound kiln method. The characteristics of both biochar samples were estimated by using different physico-chemical methods and various analytical techniques that reveals the different elemental and structural composition of biochar. The different techniques used in the present study was Field Emission scanning electron microscope (FESEM), Energy dispersive x-ray analysis (EDX), Fourier Transmission-Infrared Radiation (FTIR), X-ray Diffraction (XRD), Thermal gravimetric analysis (TGA), Flame photometer, Total organic carbon analyser (TOC) and Solid sample module (SSM). Both biochar samples were alkaline in nature with different elemental composition. The FTIR analysis identified the functional groups of some aromatic hydrocarbons along with few alkenes, carbonyl groups and aliphatic stretching vibrations. The morphology of the biochar indicated a microporous surface. The overall structure of both biochar's was amorphous in nature which confirms the presence of crystalline carbon materials.

KEYWORDS: Biochar, analytical techniques, elemental and structural composition.

*Corresponding author

Praveen Sharma

Professor, Department of Environment Science and Engineering,

Guru Jambheshwar University, Hisar,

Contact No. 01662-263153, Haryana, India

E.mail- ps.enbt@gmail.com

1. INTRODUCTION

"Biochar as a carbon-rich source obtained from different feedstocks (wood, manure, sewage waste and plant leaves) is heated in a closed container at low oxygen conditions" [1, 2, 3, 4]. Biochar feedstock has been grouped into three categories: 1. Agricultural residues, 2. Food processing industry residues and 3.Other potential feedstock. Agricultural residues are the by-products of crop production and generated within farmland. The waste organic matter or raw materials produced from agricultural land that does not find any other application has to be discarded by the farmers. This cropland and other feedstock includes wood chips, tree bark, switch grass, bagasse, press cakes from oil, wood pellets, chicken litter, dairy manure, crop residues, sewage sludge, juice industry waste, paper sludge, tree cutting, municipal organic waste and anaerobic digesters waste [4]. Furthermore, food processing industry residues are considered as by-products of processing industry, which are normally produced outside the farmland [5].

The primary properties of biochar are directly influenced by the feedstock type and production conditions. The secondary properties of biochar are factors of its primary properties. Both the primary and secondary properties of biochar facilitate different applications [5]. The amendment of this feedstock with soil significantly improves soil quality as well as crop production [6]. Type of raw material used and the temperature conditions during pyrolysis, are the two main factors that affects the size and structure of biochar and its application on the environment [7]. High pyrolysis temperature (HPT) generally helps in the production of biochar with high surface area and high pH value. This helps in the sorption of both organic and inorganic contaminants present in soil by enhancing their micro-porosity and hydrophobicity [4, 8]. The pyrolysis at very high temperature may collapse some of the biochar pores and reduce its surface area [9]. On the other hand, biochar produced at low temperatures are more applicable for removing polar organic and inorganic contaminants by oxygen-containing functional groups, high precipitation rate, and electrostatic attraction [10]. The degree of carbonization of the raw material increases with pyrolysis temperature, which indicates the increase in carbon content and decrease in the values of hydrogen and oxygen content of the biochar [11, 12].

On the other hand, biochar produced at low production temperature (LPT), results into lower surface area and low pH value. Furthermore, LPT also results in to higher water holding capacity (WHC) and cation exchange capacity (CEC) [11, 13]. The negative surface charge on biochar attracts hydrogen ions from the soil solution which helps to increase the soil pH value [9, 14]. In some cases, the biochar produced by the thermo-chemical process may be neutral and it may vary from 4-12 [15, 16]. Like soil pH, the electrical conductivity (EC) of biochar is also associated with the ions that are soluble in water. Hence, the soil water suspension is used for EC measurement [17]. Biochar produced

at high temperature consists approximately, 95% carbon content, less than 5% oxygen content and 5-7% hydrogen content [18].

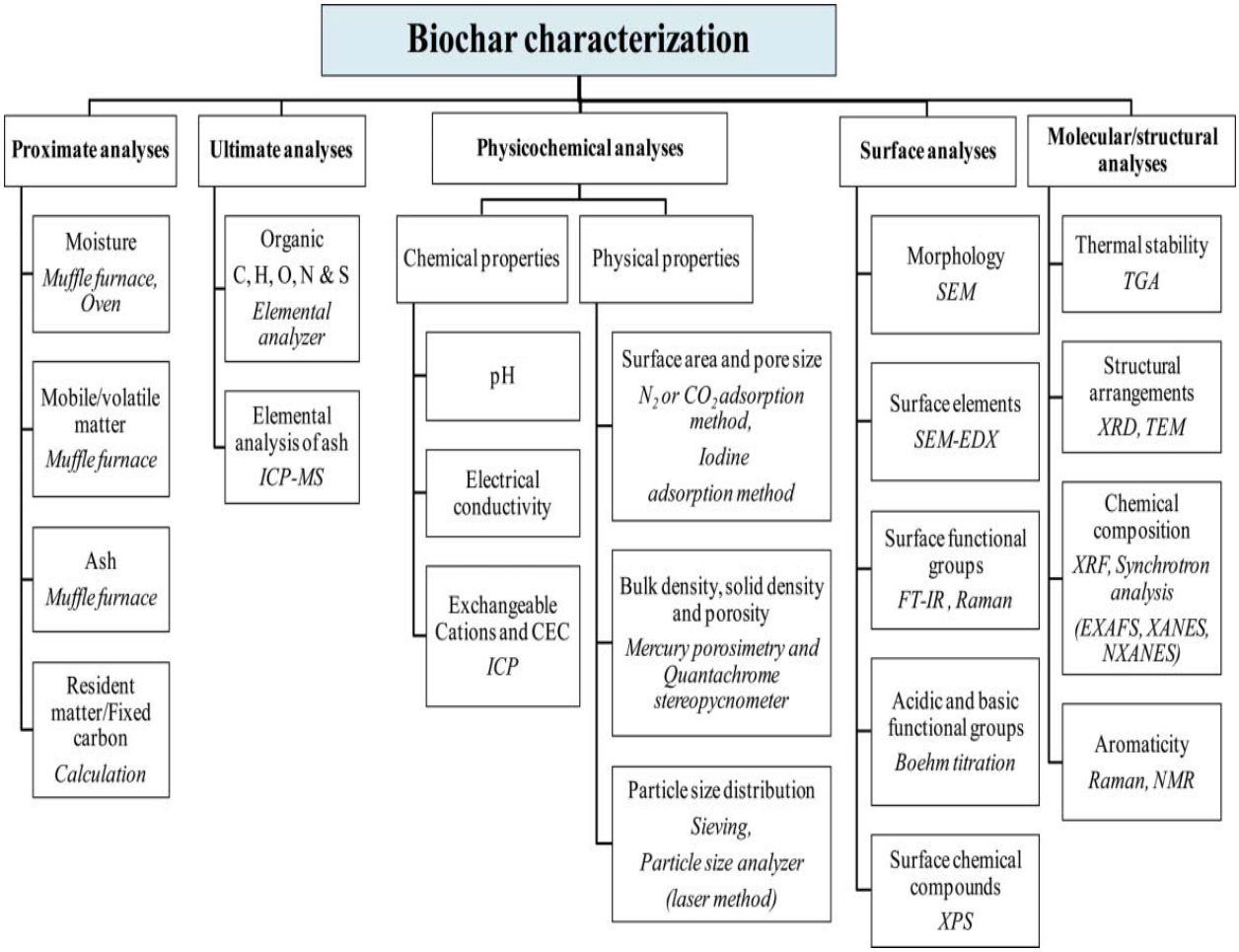

Fig. 1: Graphical representation of physico-chemical and other characteristics of biochar.

Cation exchange capacity (CEC) and exchangeable bases are one of the important parameters of soil and sediments. The CEC can be estimated by summation of exchangeable bases (Ca, Mg, Na and K). At high production temperature, the CEC was maximum due to high surface area, presence of surface negative charge and resultant affinity for soil cations. Available macro and micro nutrients present in biochar have been essential for its application in the agriculture. The amount of nutrients present in different types of biochar mainly depends on the raw material from which it is derived and the production conditions [5]. The general parameters analysed by proximate and ultimate analysis, physico-chemical analysis, surface and structural analysis were represented in Fig. 1. The structural properties of biochar changes due to the carbonization process, especially chemical structure. This happens mostly by detachment of surface functional groups that applies on bio-geochemical and

technical carbonization of biochar production. The release of hydrogen (H_2), oxygen (O_2) and other groups causes a reduction in the fixed carbon ratio.

The biochar aromaticity rapidly enhances at a temperature range between 200 to 500^{0}C and maximum is achieved at 500 and 800^{0}C. At this temperature, the whole carbon content present in biochar was bound with aromatic structure. Functional groups attached in biochar structure are mainly –COOH and –OH group, which significantly affects the soil pH. Ash content of biochar depends on the raw material used during pyrolysis process. Moreover, water and volatile matter are emitted and ash content remains present in the solid form. The amount of ash content increased with increasing treatment temperature.

All of these above properties of biochar help us to analyse the potential environmental applications of the biochar. The main objective of this research was to understand the physico-chemical characteristics of biochar derived from *Prosopis juliflora* (PJBC) and mixed wood (MWBC). This study highlights the presence of:

- Crystalline structure of the biochar.
- Alkaline, carbon rich and porous nature of the biochar.
- Different elemental and functional composition of the biochar.

2. MATERIALS & METHODS

2.1 Biochar preparation

In the proposed experimental study, different types of raw materials were used for the synthesis of biochar. The biochar derived from *Prosopis juliflora* was procured from C6 Agrisciences India private limited, Telangana, Hyderabad and mixed wood biochar (sal, cheed and teak hard wood biomass) was procured from Chorahi village, Bilaspur, Distt. Yamunanagar, Haryana, India. Both biochar's were synthesized by traditional earth mound kiln method at low production temperature 450^{o}C. Biochar sample was crushed to from a fine power and sieved through 2 mm sieve and stored in a closed air tight containers for further physico-chemical characterization.

2.2 Physico-chemical characterization of biochar

2.2.1 Volatile matter, ash and fixed carbon content

Volatile matter and ash content were analysed by using the American Society for Testing and Materials ASTM (D1762-84) method [19], which is proposed by International Biochar Initiative (IBI). The volatile matter was estimated by measuring the sample weight loss (in grams) that follows the combustion of 1 g of biochar sample in a crucible at 950°C. Following the same procedure, the ash content was determined at 750°C. Fixed-carbon content was calculated by subtracting volatile matter and ash content from the total dry weight of biochar [20, 21].

$$\text{Volatile matter (\%)} = \frac{(B - C)}{B} \times 100 \qquad \text{eq. 1}$$

Here, B= sample weight (grams) after drying at 105°C

C = sample in grams after drying at 950°C

$$\text{Ash content (\%)} = \frac{D}{B} \times 100 \qquad \text{eq. 2}$$

Here, B= sample in grams after drying at 105°C

D= residues in grams

Fixed carbon (%) = 100% - (volatile matter % + ash content %) eq.3

2.2.2 Moisture content

The muffle furnance was heated up to 750°C and placed a previously ignited crucible in furnance for 10-15 min. Cooled down the crucible in desiccator for 1 hr. Then, accurately weighed the crucible and added 1g sample and placed it in the oven at 105°C for approximately 2 hrs. Placed the dried sample in a desiccator for 1 hr and weighed it again [19].

$$\text{Moisture (\%)} = \frac{(A-B)}{A} \times 100 \qquad \text{eq. 4}$$

Here, A= air-dry sample weight in grams

B= sample in grams after drying at 105°C

2.2.3 Elemental composition

The elemental composition of biochar (C, H, N, O, Mg, Si, K, Ca, Cr, Fe, Ni, Cu, Mn and Zn) was determined by using Energy-dispersive X-ray spectroscopy (Thermo Scientific, FLASH 2000) microprocessor based instrument.

2.2.4 Thermal analysis

The thermal stability analysis of both samples was performed by using a TGA/DSC 3+ STAR^e System (Mettler Toledo), heated up to 600°C with 15°C/min heating rate under air atmosphere (gas type). The non-combustible component was determined as the weight left after thermal combustion at 600°C relative to the starting biochar weight.

2.2.5 Fourier Transform Infrared Spectrophotometer (FTIR)

FTIR is the most powerful technique for the determination of different functional groups present in the sample. For FTIR analysis, 10 mg of dried powder of biochar was encapsulated in 100 mg of KBr pellet. The biochar and KBr powder was then re-ground in a mortar and pestle to ensure homogeneity. This powder was further used for the preparation of translucent sample discs or pellet. This pellet was pressed at 10 MPa of pressure. The pellet was then loaded in FTIR spectroscope

(Spectrum BX, Perkin Elmer, USA), with a scanning range from 400 to 4000 cm^{-1} and resolution of 4 cm^{-1}.

The following broad-band assignment was used, O–H stretching vibrations of hydroxyl groups (alcohols, phenols and organic acids) ranged from 3400 to 3410 cm^{-1}, C–H stretching of alkyl structures at 2850 to 2950 cm^{-1}, COO- asymmetric stretching at 1580 to 1590 cm^{-1}, C–H deformation of CH_3 group at 1460 cm^{-1}, O–H stretching of phenolic compounds ranged from 1280–1270 cm^{-1}, and three bands lies at the range of 460, 800 and 1000–1100 cm^{-1} showed the stretching of Si–O [22, 23, 24].

2.2.6 pH and EC

The pH and EC of biochar samples were determined in a ratio of 1:10 (w/v) (2g sample was dissolved in 20 ml de-ionized water), kept it for 1hr in orbital shaker for proper mixing. The pH was measured by using electrode type pH meter (Cyberscan pH tutor, EUTECH). Now, centrifuged the sample for 10-15 minutes and supernatant was used for measuring EC by using conductivity meter.

2.2.7 Cation exchange capacity (CEC) & Total organic carbon content (TOC)

CEC was determined by using Flame photometer (ELICO CL-378). TOC, TC and IC were analysed by using the Total Organic Carbon Analyser and Solid Sample Module (TOC-L Analyser & SSM-5000A (Shimadzu Corporation).

$$TOC = TC - IC \qquad \text{eq. 5}$$

2.2.8 XRD

X-Ray Diffraction (XRD) analysis was carried out to study the crystallographic structure of compound by using a computer-controlled X-ray diffractometer (Bruker- D8 Advance, Germany) equipped with a stepping motor and graphite crystal monochromator.

2.2.9 FESEM

The surface morphology and porous structure of the biochar was characterized by using FESEM. Biochar's were held onto an adhesive carbon tape on an aluminum stub followed by sputter coating with gold to achieve good visibility of the images prior to viewing. Images were taken at 15 kV with a JSM-6360 model FESEM.

3. RESULTS & DISCUSSION

3.1 Physico-chemical characterization of biochar

Characteristics of biochar derived from *Prosopis juliflora* (PJBC) and mixed wood (MWBC) raw material are shown in Table. 1. Mixed wood biochar showed maximum water holding capacity as compared to *Prosopis juliflora* biochar. This was due to the presence of highly porous structure of MWBC which was clearly showed in different images of FESEM (Fig. 5. g, h, I, j, k, l). WHC of

biochar was affected by the average pore diameter and the total pore volume. The presence of large pores in biochar cannot only hold the maximum water in it, but also acts as the passage for small pores [25]. Cation exchange capacity (CEC) was also high in case of MWBC due to the holding of maximum exchangeable bases in MWBC as compared to PJBC. The pH, EC values and total Na content in both biochar samples were corresponding to each other. Total organic carbon content was maximum in case of PJBC as compared to MWBC.

Table. 1: "Biochar characteristics used in the experiment".

Sr. No.	Characteristics	PJBC	MWBC
1.	Water holding capacity (%)	93	107
2.	pH (1:10 solid water suspension)	8.54	8.59
3.	Electrical conductivity (EC) ds/m (1:10 soil water extract)	1.43	1.41
4.	Cation exchange capacity (cmol/kg)	16.9	19.5
5.	Total organic carbon (g Kg^{-1})	870	655
6.	Total Na (g Kg^{-1})	0.68	0.71

Here, PJBC= *Prosopis juliflora* biochar and MWBC= mixed wood biochar, (all Values are mean of triplicate samples).

3.2 Proximate and ultimate analysis of biochar

The biochar derived from mixed wood plant material showed maximum value for volatile and ash content as compared to PJBC (Table. 2). This may be due to maximum partial changes and interactions between organic and inorganic constituents of different raw materials used during mixed wood biochar production. The ultimate or elemental compositions of both biochar samples prepared at 450°C are shown in Fig. 2. Energy Dispersive X-Ray analysis (EDX) is an X-Ray technique which is used to identify the elemental composition of PJBC and MWBC.

Table. 2: "Proximate and Ultimate analysis of biochar derived from *Prosopis juliflora* and mixed wood plant biomass".

Sr. No.	**Constituents**	**PJBC**	**MWBC**
Proximate Analysis			
1.	Moisture (%)	0.5	0.97
2.	Volatile Matter (%)	11.01	14.86
3.	Ash content (%)	5.2	7.98
4.	Fixed carbon (%)	83.29	76.19
Ultimate Analysis			
5.	Hydrogen (%)	1.01	1.71
6.	Sulfur (%)	0.13	0.03
7.	Oxygen (%)	14.51	20.26
8.	Nitrogen (%)	1.07	1.67

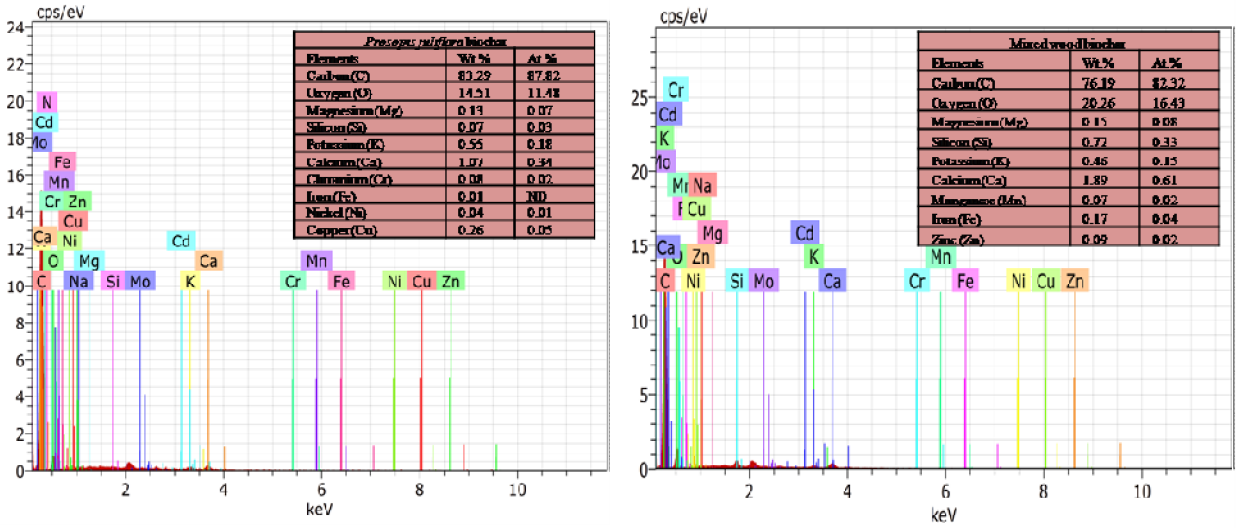

Fig. 2: Represents the EDX spectra of (1) *Prosopis juliflora* and (2) Mixed wood biochar.

The data obtained by EDX analysis consists of a spectrum which highlights the distribution of various elements present in the sample and same can be analysed by different coloured peaks. Silicon (Si) was present in the form of SiO_2 in both biochar samples [26]. The maximum fixed carbon content was observed in *Prosopis juliflora* biochar as compared to mixed wood biochar i.e. 83.29% and 76.19%, respectively. Other constituents like H, N, O and S are shown in Table. 2. The values of other parameters like total Na, K, Mg, Ca, Mn, Zn and Fe were approximately similar in both biochar samples analysed by EDX. Furthermore, the smallest amount of Ni and Cu was detected only in PJBC.

3.3 XRD Analysis

Prosopis juliflora and mixed wood biochar was pyrolysed at low temperature (450°C) under oxygen-limited conditions. The X-Ray diffraction patterns of biochar samples are illustrated in Fig. 3. The strong and sharp peak maxima at approximately, 2θ= 26.8° in *Prosopis juliflora* biochar is due to SiO_2 (quartz). Another sharp peak at 29° in both biochar samples was due to $CaCO_3$ (calcite). These sharp peaks indicate the higher degree of orientation and presence of crystalline carbon structure. The small and narrow peak found at 38.8° in both biochar samples was due to CaO (lime). Peak at 50° is due to $Ca(OH)_2$ and at 65° shows the presence of MnO_2. The small peak at approximately 67.8° in *Prosopis juliflora* was due to occurrence of Al_2O_3. These results were closely in-line with [27, 28]. A narrow peak at 2θ= 21° in *Prosopis juliflora* and at 40° in both biochar's, was due to the presence of some MgO and $CaCO_3$ mineral crystals in the sample.

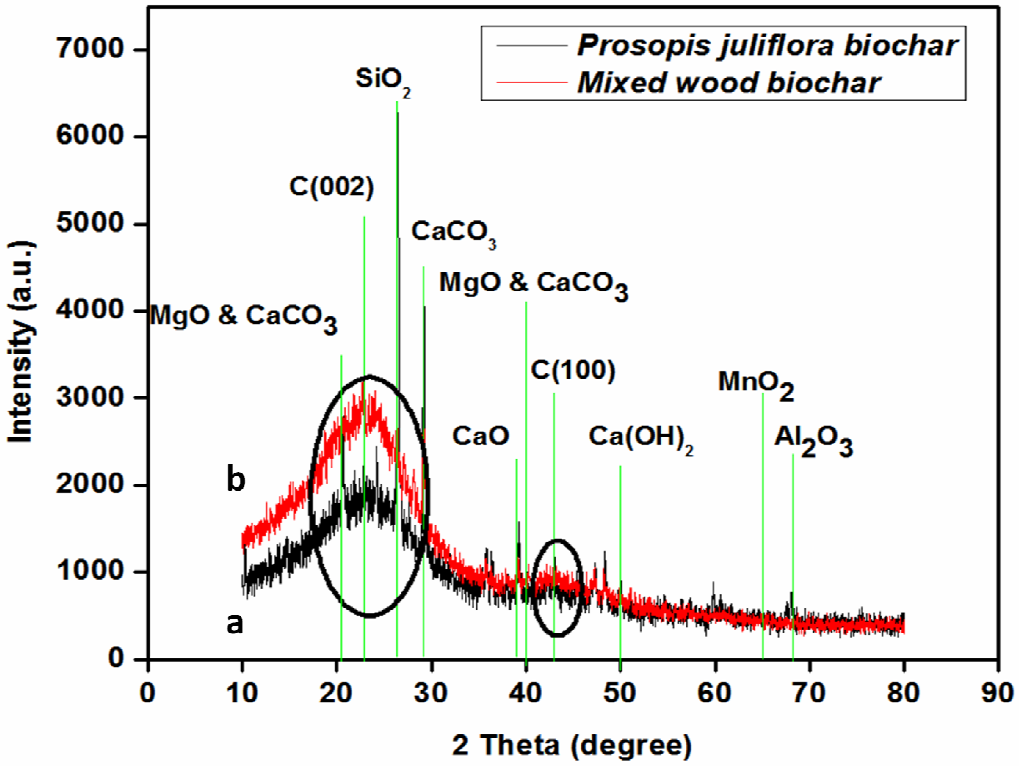

Fig. 3: Showed the XRD spectra of (a) *Prosopis juliflora* and (b) Mixed wood biochar.

The occurrence of broad peak around 18° to 30° in both biochar samples prepared at low temperature indicated the presence of a crystalline plane index C(002). This C(002) crystal plane was due to azimuthal and parallel orientation of the aromatic and partially carbonized layer. Similarly, another broad peak was found in the range of approximately 42° to 46° in both biochar samples. This happens due to crystal plane index of C(100), which indicates the presence of condensed aromatic carbonized patterns. These results were in close proximity with [28, 29, 30]. Thus, the X-Ray diffraction analysis confirmed the presence of crystalline carbon materials.

3.4 FTIR Analysis

FTIR technique is used to obtain an infrared spectrum of emission or absorption of a gas, liquid or solid samples. In the present study, FTIR spectra of *Prosopis juliflora* and mixed wood biochar were analysed (as shown in Fig. 4). This spectrum showed that the similar broad peaks were found in case of both biochar samples in the region from 3000–4000 cm^{-1}. This region is attributed to –OH group stretching band present in both inorganic and organic components (Si–OH) of biochar. Small peak at 2929.34 cm^{-1} in both samples are assigned to C–H aliphatic stretching vibration [31]. Spectral vibrations at 2359.4 cm^{-1} was due to the presence of CO_2 group [28]. A region between 2000-

2400 cm^{-1} corresponds to O=C=O, –C≡C– and –C≡N stretching [28, 32]. Moreover, absorption frequencies of different functional groups were also shown in Table.3.

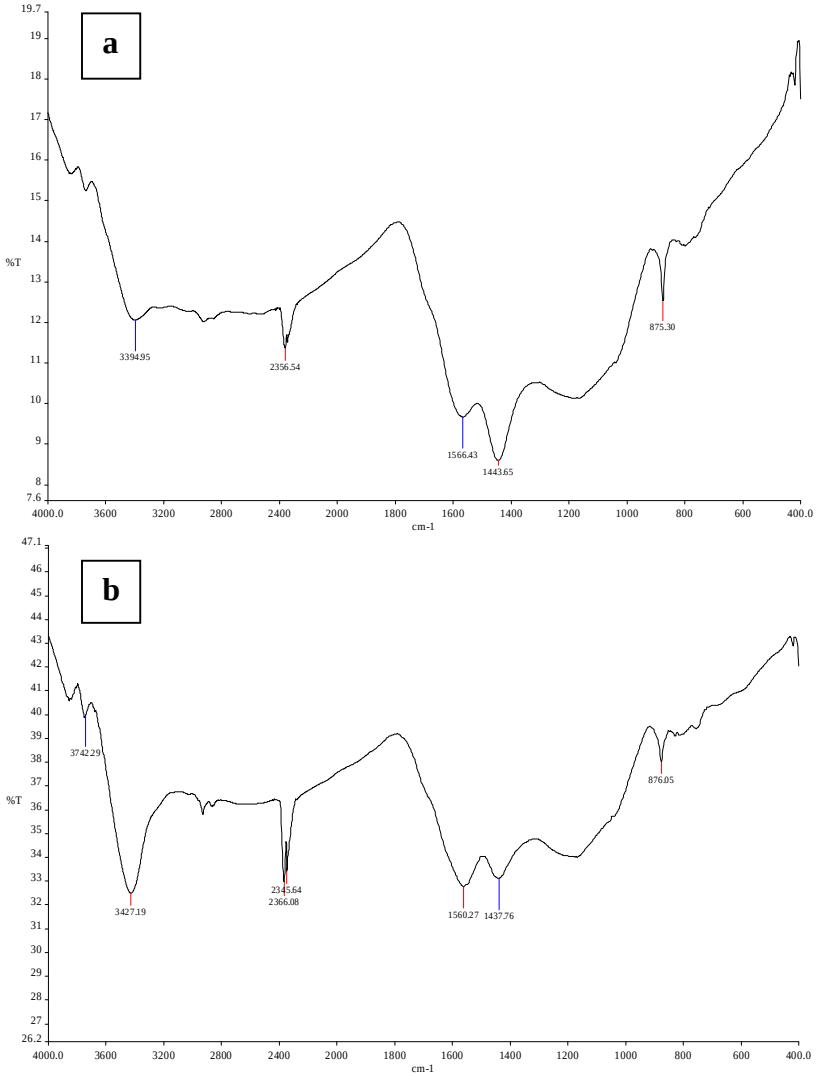

Fig. 4: Showed the FTIR spectra of (a) *Prosopis juliflora* and (b) Mixed wood biochar.

Table. 3: "Functional groups of the biochar samples according to FTIR spectra".

(adopted from [33])

Sr. No.	Wavelength (cm-1)	Functional groups	Compounds
1.	490-620	C–I	Halogen
2.	500-1400	C–F, C–Br, C–Cl, C–I	Alkyl halides
3.	500	C–I	Alkyl halide
4.	500-600	C–Br	Alkyl halide
5.	600-800	C–Cl	Alkyl halide
6.	615-620	C-H	aromatic
7.	625-830	C=C	Alkenes and aromatic compounds
8.	630-750	C=C	Amino and aromatic compounds
9.	675-1000	C–H	Alkenes
10.	750-900	O–H	Aromatics

11.	1000-1300 & 911-1150	C–O	Ether
12.	1000-1400	C–F	Alkyl halide
13.	1080-1360	C–N	Amine
14.	1115-1130	C-O-C	Etheric
15.	1385	C-C	Aromatic
16.	1400-1600	C=C	Aromatic
17.	1458-1591	C_6H_5OH	Phenol ring
18.	1515-1560 & 1345-1385	N–O	Nitro
19.	1600	N–H	Amine
20.	1620-1680	C=C	Alkene
21.	1610-1632, 1670-1820 & 1725-1745	C=O	Carbonyl
22.	2854-2926	CH4	Methyl group
23.	2850-3000	C–H	Alkane
24.	2210-2260	C–N	Nitrile
25.	3300	C–H	Alkyne
26.	3300-3500	N–H	Amine
27.	3200-3600 & 3500-3700	O–H	Hydroxyl

The small peak at 1555 cm^{-1} in both biochar samples was attributed to –C=C– bond stretching and –C=O stretching of aromatic rings. The sharp and narrow peak at 874.8 cm^{-1} in both samples was due to Si-O_4 band vibration or it may be due to –CH bonding of aldehyde functional groups. The peak at 469 cm^{-1} was due to bending vibrations of Si-O-Si [33]. An aliphatic –C–H stretching was observed at 2929.3 cm^{-1} which confirmed that biochar cellulose content is not entirely carbonized during pyrolysis [34]. The medium peak found at 1590 and 2352 cm^{-1} represented the deformation and stretching due to occurrence of –NH (amine) functional group [35].

3.5 Field- emission scanning electron microscopy (FESAM)

FESEM monographs of PJBC and MWBC illustrates the highly porous structure and surface morphology of biochar. The xylem structure and biochar surface porosity was clearly shown in both biochar samples (as represented by different images in Fig. 5). The working distance of these images was approximately 8.0 mm, with 5.0 KV high voltages and resolution power (µm) varies at different scales. Generally, biochar retains the biomass cell wall structure, which changes with feedstock type and production conditions [36].

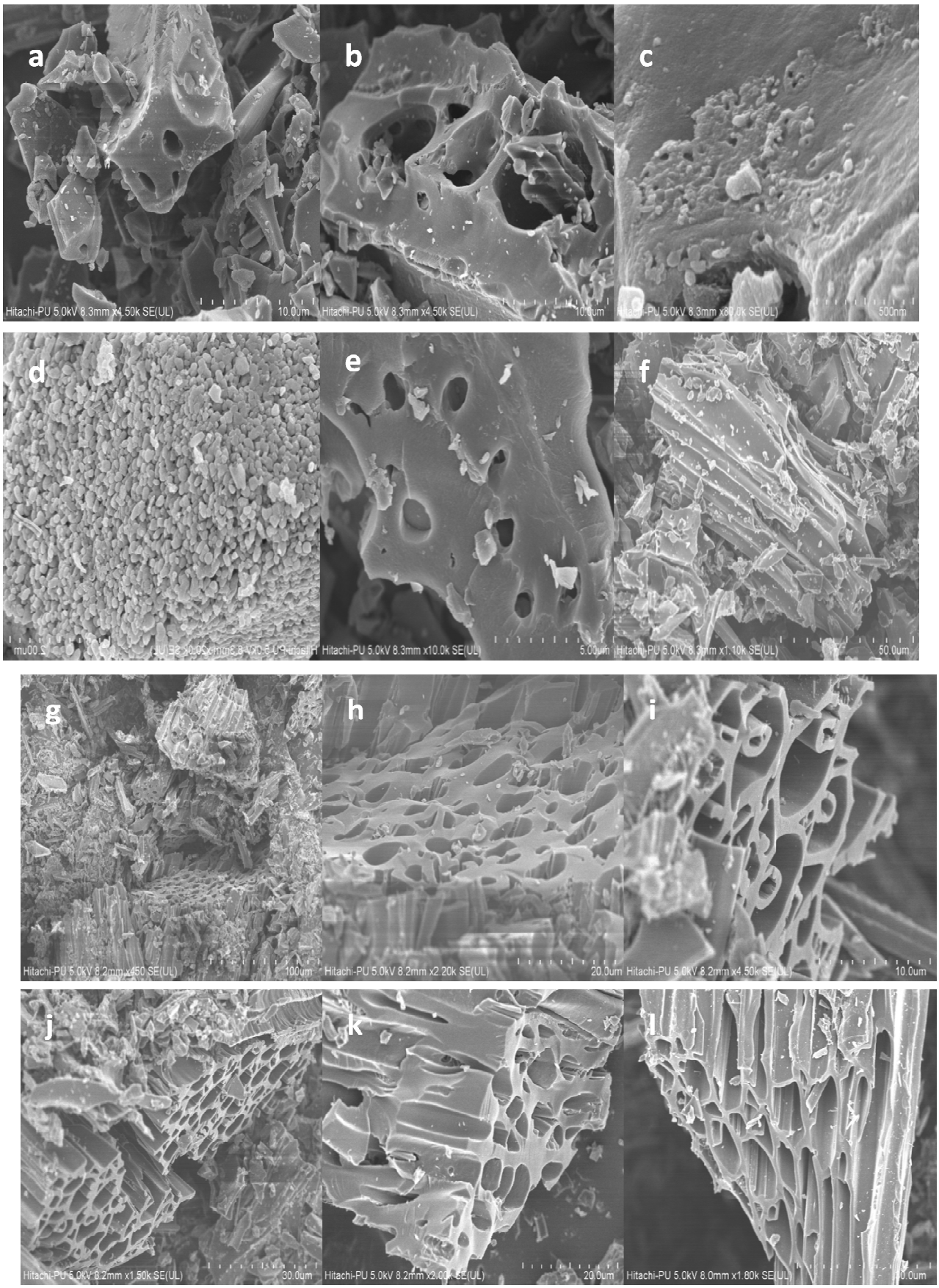

Fig. 5: Represents the surface morphology and porosity of *Prosopis juliflora* (a, b, c, d, e, f) and Mixed wood biochar (g, h, I, j, k, l).

3.6 Thermogravimetric analysis of biochar

Thermogravimetric analysis (TGA) is a useful method to examine the structure of biochar derived from different feedstock types [23, 37]. In the present research, both biochar samples showed similar thermal degradation profile (as represented in Fig. 6). The 0°C was used as the starting point for plotting TGA curves. Slight weight loss was observed, when heating temperature was applied in the range between 25 to 100°C. This was due to the loss of water from the biochar samples. After this, the curve became stable until 300°C. In the present research it was found that, no phase change was observed in both biochar samples at the range between 100-300°C, which indicates that at this temperature range no decomposition occurred.

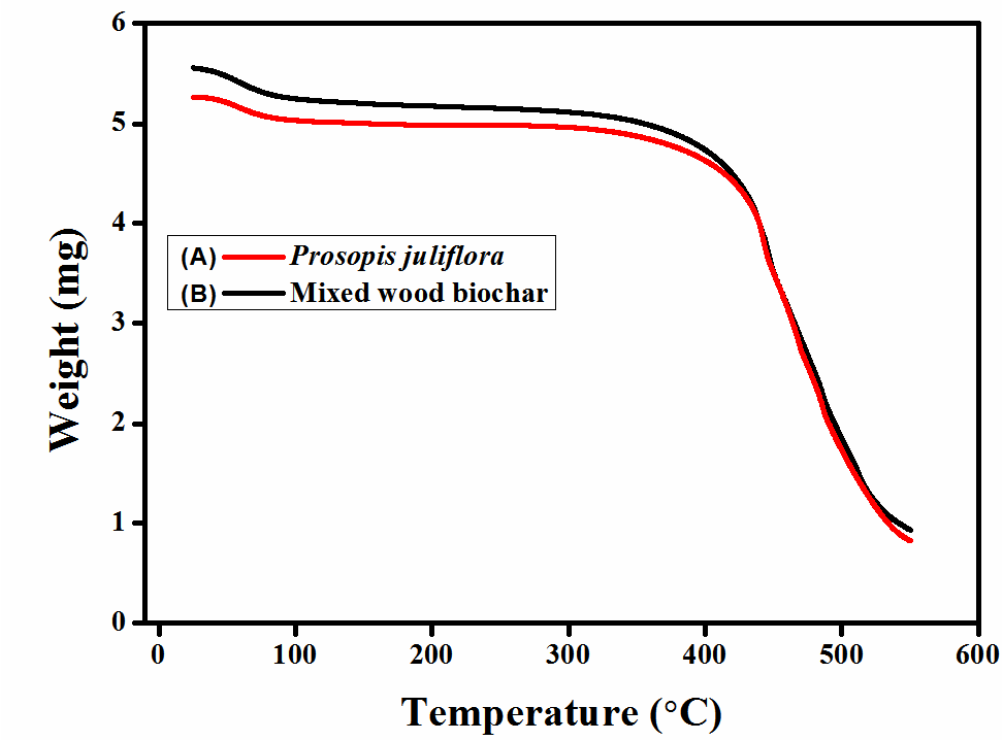

Fig. 6: Thermogravimetric curves of biochar's derived from (A) *Prosopis juliflora* and (B) Mixed wood.

The weight loss proportion was increased with pyrolysis temperature up to 550°C. The weight loss of PJBC and MWBC was observed to be 80.98% and 81.98% of the total weight, respectively. At higher temperature range, the biochar samples became more stable or more resistant to decomposition. These results are closely in-line with [11, 20]. The loss of thermal conductivity of biochar samples corresponding to their parent biomass was due to the formation of a porous structure [18].

CONCLUSIONS

Biochar can be synthesized from a wide range of different forest and agricultural raw materials at different pyrolysis conditions. The physical and chemical characteristic of biochar helps to identify the basic structural and elemental composition of the biochar. Biomass consists of

cellulose, hemicelluloses and lignin content. Most part of the cellulose and hemicelluloses are broken down during pyrolysis at temperature range between 200-300°C (known as torrefaction). A torrefaction occures at this temperature range is a highly sensitive process and it helps to provide a better fuel quality for gasification and combustion. The relative carbon (C) content was enhanced as the oxygen (O) and hydrogen (H) contents were reduced in the biochar and dependence nature of nitrogen (N) content was yet not clear. Further, devolatilization significantly increased the ash content by removing all volatile components from the solid biomass and yielding highly efficient char. This char consisted small residues of O, N, H and higher amount of C content. Moreover, the amount of fixed carbon and energy content increases with temperature range. The presence of few functional groups during pyrolysis process, leads to an increase in the pH value of the biochar.

Devolatilization of gases from char developed a surface porous structure. This porous structure directly influences other properties of the biochar like density, WHC, mechanical stability and CEC. The rate of porosity increases with carbonization. At very high pyrolysis temperature, porosity decreases and density increases or vice-versa. FESEM results clearly showed the porous nature of both biochar's. Further, XRD analysis explained the crystallinity of biochar derived from different feedstock types. Both biochar's (PJ and MW) showed good potential for WHC and CEC. Furthermore, research in this direction would be helpful to establish and explore full potential of biochar derived from different raw materials as a technology with their multidisciplinary applications for environment.

ACKNOWLEDGMENT

Author Varinder Kaur is highly thankful to the "Maulana Azad National Fellowship for Minority Students" formulated and funded by the Ministry of Minority Affairs and UGC-SAP for financial assistance.

REFERENCE'S

1. Huang D, Liu L, Zeng G, Xu P, Huang C, Deng L, Wang R, Wan J. The effects of rice straw biochar on indigenous microbial community and enzymes activity in heavy metal-contaminated sediment. Chemosphere. 2017; 174:545-53. https://doi.org/10.1016/j.chemosphere.2017.01.130.
2. Lehmann J, Joseph S. Biochar for environmental management: an introduction, in: L. Johannes, J. Stephen (Eds.), Biochar for environmental management: science and technology. Earthscan- publishing Inc., London, 2009; 978-1.

3. Rutigliano FA, Romano M, Marzaioli R, Baglivo I, Baronti S, Miglietta F, Castaldi S. Effect of biochar addition on soil microbial community in a wheat crop. European Journal of Soil Biology. 2014; 60:9-15. https://doi.org/10.1016/j.ejsobi.2013.10.007.
4. Zhang C, Liu L, Zhao M, Rong H, Xu Y. The environmental characteristics and applications of biochar. Environmental Science and Pollution Research. 2018; 25(22):21525-34. https://doi.org/10.1007/s11356-018-2521-1.
5. Igalavithana AD, Mandal S, Niazi NK, Vithanage M, Parikh SJ, Mukome FN, Rizwan M, Oleszczuk P, Al-Wabel M, Bolan N, Tsang DC. Advances and future directions of biochar characterization methods and applications. Critical reviews in environmental science and technology. 2017; 47(23):2275-330. https://doi.org/10.1080/10643389.2017.1421844.
6. Parmar A, Nema PK, Agarwal T. Biochar production from agro-food industry residues: a sustainable approach for soil and environmental management. Current Science. 2014; 107(10):1673-82. http://www.currentscience.ac.in/Volumes/107/10/167.
7. Woolf D, Amonette JE, Street-Perrott FA, Lehmann J, Joseph S. Sustainable biochar to mitigate global climate change. Nature communications. 2010; 1:56. https://doi.org/10.1038/ncomms1053.
8. Ahmad M, Rajapaksha AU, Lim JE, Zhang M, Bolan N, Mohan D, Vithanage M, Lee SS, Ok YS. Biochar as a sorbent for contaminant management in soil and water: a review. Chemosphere. 2014; 99:19-33. https://doi.org/10.1016/j.chemosphere.2013.10.071.
9. Tang J, Zhu W, Kookana R, Katayama A. Characteristics of biochar and its application in remediation of contaminated soil. Journal of bioscience and bioengineering. 2013; 116(6):653-9. https://doi.org/10.1016/j.jbiosc.2013.05.035.
10. Sizmur T, Quilliam R, Puga AP, Moreno-Jiménez E, Beesley L, Gomez-Eyles JL. Application of biochar for soil remediation. Agricultural and environmental applications of biochar: Advances and barriers. 2016; 295-324. https://doi:10.2136/sssaspecpub63.2014.0046.5.
11. Wang S, Gao B, Li Y, Mosa A, Zimmerman AR, Ma LQ, Harris WG, Migliaccio KW. Manganese oxide-modified biochars: preparation, characterization, and sorption of arsenate and lead. Bioresource technology. 2015; 181:13-7. https://doi.org/10.1016/j.biortech.2015.01.044.
12. Uchimiya M, Klasson KT, Wartelle LH, Lima IM. Influence of soil properties on heavy metal sequestration by biochar amendment: 1. Copper sorption isotherms and the release of cations. Chemosphere. 2011; 82(10):1431-7. https://doi.org/10.1016/j.chemosphere.2010.11.050.

13. Ippolito JA, Laird DA, Busscher WJ. Environmental benefits of biochar. Journal of environmental quality. 2012; 41(4):967-72.https://doi:10.2134/jeq2012.0151

14. Latawiec A, Królczyk J, Kuboń M, Szwedziak K, Drosik A, Polańczyk E, Grotkiewicz K, Strassburg B. Willingness to adopt biochar in agriculture: The producer's perspective. Sustainability. 2017; 9(4):655. https://doi.org/10.3390/su9040655.
15. Lehmann J. A handful of carbon. Nature. 2007; 447(7141):143. https://doi.org/10.1038/447143a.
16. Chan KY, Zhihong X. Biochar: nutrient properties and their enhancement, in: L. Johannes, J. Stephen (1st Eds.), Biochar for environmental management: science and technology. Earthscan-publishing Inc., U.K, 2009; 67-84.
17. Rajkovich S, Enders A, Hanley K, Hyland C, Zimmerman AR, Lehmann J. Corn growth and nitrogen nutrition after additions of biochars with varying properties to a temperate soil. Biology and Fertility of Soils. 2012; 48(3):271-84. https://doi.org/10.1007/s00374-011-0624-7.
18. Weber K, Quicker P. Properties of biochar. Fuel. 2018; 217:240-61. https://doi.org/10.1016/j.fuel.2017.12.054.
19. Standard Test Method for Chemical Analysis of Wood Charcoal. ASTM International, West Conshohocken, PA, 2007, https://www.astm.org/DATABASE.CART/HISTORICAL/D1762-84R07.htm (ASTM D1762-84 (2007).
20. Sun J, He F, Pan Y, Zhang Z. Effects of pyrolysis temperature and residence time on physicochemical properties of different biochar types. Acta Agriculturae Scandinavica, Section B- Soil & Plant Science. 2017; 67(1):12-22. https://doi.org/10.1080/09064710.2016.1214745.
21. Zhao SX, Ta N, Wang XD. Effect of temperature on the structural and physicochemical properties of biochar with apple tree branches as feedstock material. Energies. 2017;10(9): 1293. https://doi.org/10.3390/en10091293.
22. Guo J, Chen B. Insights on the molecular mechanism for the recalcitrance of biochars: interactive effects of carbon and silicon components. Environmental Science & Technology. 2014; 48(16):9103-12. https://doi.org/10.1021/es405647e.
23. Jindo K, Mizumoto H, Sawada Y, Sanchez-Monedero MA, Sonoki T. Physical and chemical characterization of biochars derived from different agricultural residues. Biogeosciences. 2014; 11(23):6613-21. https://doi.org/10.5194/bg-11-6613-2014.

24. Wu W, Yang M, Feng Q, McGrouther K, Wang H, Lu H, Chen Y. Chemical characterization of rice straw-derived biochar for soil amendment. Biomass and bioenergy. 2012; 47:268-76. https://doi.org/10.1016/j.biombioe.2012.09.034.
25. Zhang J, You C. Water holding capacity and absorption properties of wood chars. Energy & Fuels. 2013; 27(5):2643-8. https://doi.org/10.1021/ef4000769.
26. Ma X, Zhou B, Budai A, Jeng A, Hao X, Wei D, Zhang Y, Rasse D. Study of biochar properties by scanning electron microscope–energy dispersive X-ray spectroscopy (SEM-EDX). Communications in Soil Science and Plant Analysis. 2016; 47(5):593-601. https://doi.org/10.1080/00103624.2016.1146742.
27. Manikandan A, Subramanian KS. Ability of Urea Impregnated Biochar Fertilizers For Securing the Slow Release of Nitrogen in Soils–Preliminary Study. International Journal of Agriculture Sciences, ISSN. 2015:0975-3710.
28. Mohan D, Abhishek K, Sarswat A, Patel M, Singh P, Pittman CU. Biochar production and applications in soil fertility and carbon sequestration–a sustainable solution to crop-residue burning in India. Rsc Advances. 2018; 8(1):508-20. http:// doi.org/10.1039/c7ra10353k.
29. Cao X, Harris W. Properties of dairy-manure-derived biochar pertinent to its potential use in remediation. Bioresource technology. 2010; 101(14):5222-8. https://doi.org/10.1016/j.biortech.2010.02.052.
30. Chen D, Yu X, Song C, Pang X, Huang J, Li Y. Effect of pyrolysis temperature on the chemical oxidation stability of bamboo biochar. Bioresource technology. 2016; 218:1303-6. https://doi.org/10.1016/j.biortech.2016.07.112.
31. Pongpiachan S. FTIR spectra of organic functional group compositions in PM2.5 collected at Chiang-Mai City, Thailand during the haze episode in March 2012. Journal of Applied Sciences. 2014; 14(22):2967-77. https://doi.org/10.3923/jas.2014.2967.2977.
32. Figueiredo C, Lopes H, Coser T, Vale A, Busato J, Aguiar N, Novotny E, Canellas L. Influence of pyrolysis temperature on chemical and physical properties of biochar from sewage sludge. Archives of Agronomy and Soil Science. 2018; 64(6):881-9. https://doi.org/10.1080/03650340.2017.1407870.
33. Saikia BK, Boruah RK, Gogoi PK, Baruah BP. A thermal investigation on coals from Assam (India). Fuel Processing Technology. 2009; 90(2):196-203.https://doi.org/10.1016/j.fuproc.2008.09.007.
34. Chia CH, Downie A, Munroe P. Characteristics of biochar: physical and structural properties. Biochar for Environmental Management: Science and Technology 2nd edn, Earthscan Books Ltd: London. 2015; 20:89-109.

35. Angalaeeswari K, Kamaludeen SP. Utilization of mesquite (*Prosopis juliflora*) wood biochar for adsorption of nickel ions in aqueous solution. Int J Chem Stud. 2017; 5:687-90. http://www.chemijournal.com/archives/2017/vol5issue4/PartK/5-3-166-726.pdf
36. Gokila B, Baskar K. Characterization of *Prosofis juliflora* L. biochar and its influence of soil fertility on maize in alfisols. Int. J. Plant Animal Env. Sci. 2015; 5(1):123-7. http://www.ijpaes.com/admin/php/uploads/761_pdf.pdf.
37. Kalderis D, Kotti MS, Méndez A, Gascó G. Characterization of hydrochars produced by hydrothermal carbonization of rice husk. Solid Earth. 2014; 5(1):477-83. https://doi:10.5194/se-5-477-2014.